J Mater Sci (2009) 44:5644–5653
DOI 10.1007/s10853-009-3795-y

Mold-filling characteristics and solidification behavior of magnesium alloy in vacuum suction casting process

Haitao Teng · Tingju Li · Xiaoli Zhang · Fudong Bai · Kai Qi

Received: 8 April 2009 / Accepted: 5 August 2009 / Published online: 15 August 2009

Abstract A novel semi-solid processing technique, called new vacuum suction casting (NVSC), is used to manufacture high-quality components of AZ91D Mg alloy directly from a liquid metal. The resulting apparent morphologies and microstructures of castings are characterized in detail and linked to the corresponding mold-filling behavior and subsequent solidification behavior. It is revealed that the semi-solid metal (SSM) with higher viscosity can be caused to fill the mold with "solid-front fill", as compared with the liquid metal "spraying" in the conventional vacuum suction casting (CVSC) process. The smooth filling achieved in the NVSC process diminishes some disadvantages inherent for the CVSC sheets, and generates castings with better surface finish and structures with high integrity. The microstructure of the CVSC sheet consists of the fine and homogeneous supersaturated α-Mg solid solution due to the extremely high cooling rate. In the NVSC microstructure, the "preexisting" primary solid particles, with the morphology of near-globules or rosettes, disperse in the homogeneous matrix consisting of fine near-equiaxed secondary α-Mg grains and fine precipitates of β-$Mg_{17}Al_{12}$ intermetallics. In addition, owing to rapid solidification, the volume fraction of the β phase in the sheets obtained by both the processes is much lower than that in the as-cast ingot.

H. Teng (✉) · T. Li (✉) · F. Bai · K. Qi
Key Laboratory for Materials Modification by Laser, Ion and Electron Beams, Ministry of Education, Dalian University of Technology, Dalian 116024, China
e-mail: seantht@yahoo.com.cn

T. Li
e-mail: tjuli@dlut.edu.cn

H. Teng · T. Li · X. Zhang · F. Bai · K. Qi
School of Materials Science and Engineering, Dalian University of Technology, Dalian 116024, China

X. Zhang
School of Materials Science and Engineering, Jiangsu University of Science and Technology, Zhenjiang 212000, China

Introduction

Magnesium and its alloys, with a number of desirable features including low density, the highest strength-to-weight ratio of any of commonly used non-ferrous and ferrous metallic materials, better damping characteristics than aluminum, well castability, and abundant resources, are thus very attractive for applications in the automotive and aeronautical industries [1–5]. Currently, conventional high-pressure die casting (HPDC) is the most frequently used and readily available casting technology for magnesium alloys, and most magnesium castings are produced with the HPDC process using either hot or cold chamber machines [1, 6–9]. However, HPDC is not suitable for the production of thick-walled parts. The main problem encountered in thick-walled sections is porosity caused by turbulent die filling and solidification shrinkage [6, 10].

Different casting processes have been under development aiming at getting rid of porosity and producing high-quality components. One of the promising technologies capable of producing high-integrity components is semi-solid metal (SSM) processing [11, 12]. The most often stated advantages of SSM processing compared with conventional die casting are the non-turbulent filling of the die, near-net shape forming, better mechanical properties, less-energy consuming, and longer die-life [11–14]. In general, conventional semi-solid forming route, involving the preparation of SSM slurry, maintenance of the slurry suspension, and the transportation of the prepared slurry to the

forming press for component shaping, requires many processing steps and additional equipments [11–14]. In order to avoid burning or severe oxidation of the Mg alloys slurry during SSM processing, considering the high reactivity of Mg alloys in the melting state, the process complexity of semi-solid casting should be reduced.

In this paper, we introduce a novel semi-solid processing technique, called new vacuum suction casting (NVSC), for manufacturing high-quality components directly from liquid AZ91D Mg alloy. In the NVSC process, a liquid alloy, whose initial temperature is controlled within a narrow range around the liquidus level, is converted into semi-solid slurry by manipulating a shear-cooling system. The outstanding feature of this investigation is attributed to the fact that the NVSC process combines the semi-solid slurry making and component forming operation into one step, therefore eliminating the need for specially prepared slurry and subsequent slurry transportation steps. For comparison, conventional vacuum suction casting (CVSC) process without shear-cooling structure has been also studied. The objective of this research is to produce Mg alloy castings by applying the CVSC and NVSC technology, and assess the apparent morphologies and microstructural features of the solidified alloy. Subsequently, an attempt is made to investigate the mold-filling characteristics and the solidification behavior of both the processes.

Experimental procedures

Commercial AZ91D alloy was used in this investigation, for which the reported solidus and liquidus temperatures are 468 and 598 °C, respectively [15, 16]. The chemical composition (in wt%) of the alloy is listed in Table 1.

Table 1 Chemical compositions of AZ91D alloy (in wt%)

Al	Zn	Mn	Cu	Fe	Ni	Si	Others each	Mg
8.9	0.63	0.27	<0.002	<0.004	<0.001	<0.02	<0.01	Balanced

The NVSC process

The NVSC process is an innovative one-step SSM processing technique which, through the use of shear-cooling structure, can manufacture near-net shape components with high integrity directly from liquid alloy without turbulence or gas entrapment. Figure 1 presents the schematic of the self-designed NVSC equipment which is composed of copper mold, crucible, thermocouple, vacuum-pumping system, and shear-cooling system, etc. The vacuum-pumping system consists of vacuum pump, vacuum tank, vacuum regulating valve and vacuum measuring instrument. Compared with the CVSC process, the major difference in the equipment of the NVSC process is the specially designed shear-cooling system, which contains casting runner, a self-rotating spiral structure and cooling channels, as shown in Fig. 1b. The spiral structure has a diameter of 10 mm, a length of about 95 mm; and the cooling channels, with a length of approximately 200 mm, are designed to cool down the molten metal to its near-liquidus range with corresponding primary solid fraction.

The AZ91D alloy was melted with stainless steel crucible in an electric resistance furnace. Prior to the NVSC investigation, the molten AZ91D alloy had to be controlled at temperature 20–30 °C above the liquidus value (i.e., about 620–630 °C). When the needle valve was turned on, the liquid alloy was rapidly cooled and transformed to the SSM slurry during the liquid metal passed through the shear-cooling casting runner, in which the cooling channels provided an enhanced heat transfer and the molten alloy was characterized by high shear rate and high intensity of turbulence. The SSM was then injected at an adequate velocity into the mold cavity. The fully solidified component was finally released from the mold. It should be noted that in order to obtain adequate inlet velocity of SSM for complete mold filling, the vacuum pressure, which could

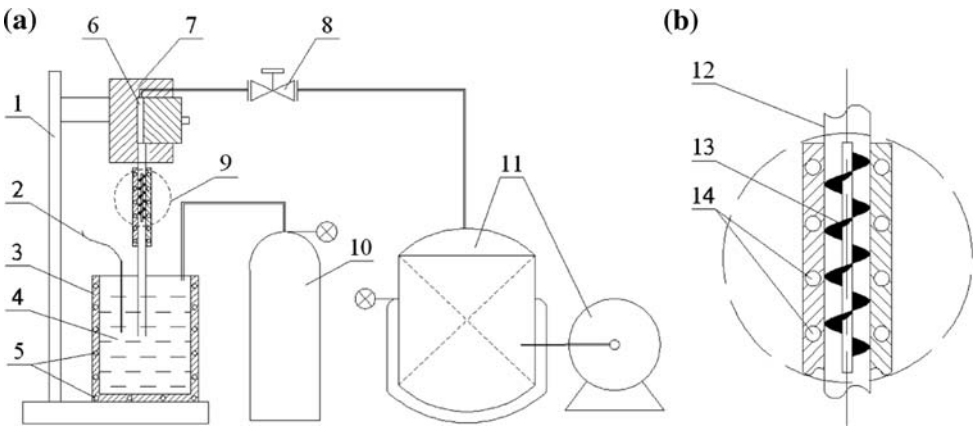

Fig. 1 Schematic illustration of the NVSC process (**a**) and the shear-cooling system (**b**): 1. fixed bracket, 2. thermocouple, 3. crucible, 4. molten metal, 5. heating elements, 6. mold cavity, 7. copper mold, 8. needle valve, 9. shear-cooling system, 10. shielding gas, 11. vacuum-pumping system, 12. casting runner, 13. spiral structure, 14. cooling channels

be changed through controlling vacuum regulating valve, in the NVSC process was much higher than that in the CVSC process. In addition, all the above procedures were conducted in a flowing protective gas (50 vol.% dry air + 50 vol.% CO_2 + 0.3 vol.% SF_6) to prevent burning and oxidation.

Measurements of specimens

The apparent morphologies of the cast sheets, including surface appearance and cross-section appearance, were observed to investigate the effects of shear cooling on mold-filling characteristics. The samples of Mg alloy cast sheet were cut and mounted into epoxy resin. Cross sections for observation were ground on silicon carbide papers, down to grit size 1200. It was followed by fine polishing with diamond, particle size from 6 to 1 μm, and etching in a 2 vol.% solution of nitric acid in ethanol. Subsequently, microstructures of etched specimens were examined by optical microscope (OM) and scanning electron microscope (SEM, JSM-5600LV). Quantitative analysis of selected microstructure characterization parameter was performed using an image analyzer. In order to obtain detailed information on the phase distribution in the specimens, phase identification was performed by X-ray diffraction (XRD, XRD-6000).

Experimental results

Apparent morphology of specimens

Figure 2 shows the surface appearances of AZ91D cast sheets produced by the CVSC process and the NVSC process at different initial temperatures. These sheets are about 35 mm in length, 15 mm in width, and 2.0 mm in thickness. Considering the very small size of the sheets and the high heat transfer rate provided by cold copper mold, the molten metal inside the mold cavity has an extremely high cooling rate. As a consequence, surface appearance of the casting can basically reflect the mold-filling characteristics of the filling alloy.

The surface appearance of the casting sheet produced by the CVSC process at the initial pouring temperature of 630 °C is shown in Fig. 2a. It exhibited numerous radial striae and jet flow traces in addition to the visible backflow zones, as pointed out by the arrows in Fig. 2a, indicating that the flow speed was very high and the mold filling was very turbulent. However, the surface quality of the sheet fabricated by the NVSC technique at 630 °C was improved significantly, as shown in Fig. 2b. The flow traces were not obvious yet and the backflow zones that were endemic to the CVSC sheets disappeared absolutely, indicating that the mold filling was laminar under the optimized processing conditions. When the initial processing temperature decreased from 630 to 620 °C, the surface appearances of the sheets were exhibited in Fig. 2c, d, in which the resulting surface appearances had similar features to those presented in Fig. 2a, b, respectively. In order to provide an additional insight into the interpretation of mold-filling behavior, the half-filled castings were produced by decreasing the vacuum pressure at 620 °C, as displayed in Fig. 3. Figure 3a shows that the liquid metal sprayed into the mold cavity and the flow was turbulent in the CVSC process. Whereas, in the NVSC process, the flow front during the injection molding was parabolic and smooth, as exhibited in Fig. 3b, which clearly showed the thixotropic character of metal alloy and the laminar mold filling.

Additionally, cross-section appearances were observed to investigate the internal quality of the cast sheets. As viewed on the cross section, we could find pores and cavities just under the surface and in the interior of the CVSC sheet (see Fig. 4a) and the porosity had a form of randomly distributed individual gaps or their clusters.

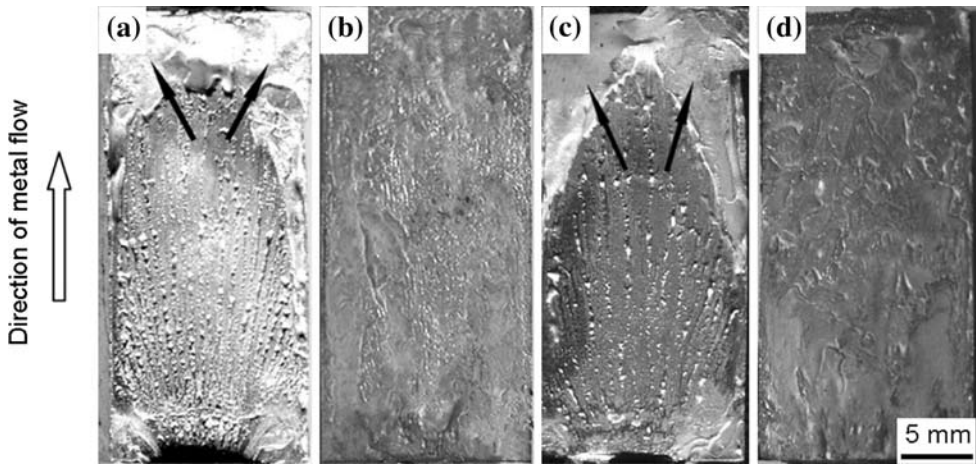

Fig. 2 Surface appearances of the sheets produced by **a** the CVSC process, at 630 °C; **b** the NVSC process, at 630 °C; **c** the CVSC process, at 620 °C; **d** the NVSC process, at 620 °C

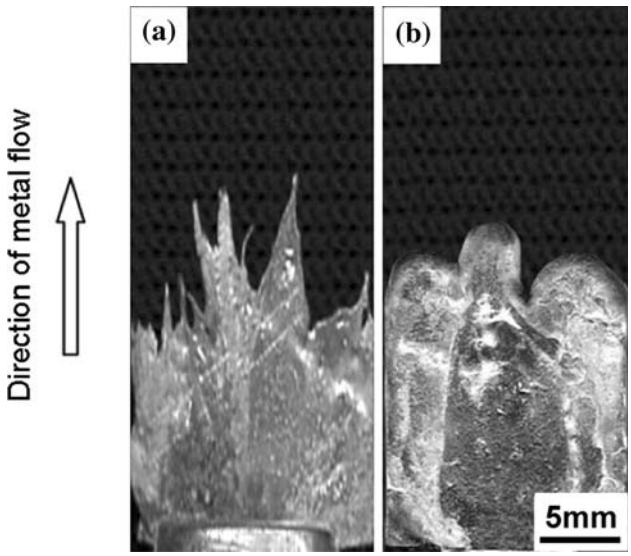

Fig. 3 Photographs of the half-filled castings showing metal flow "spraying" in the CVSC process (**a**) and laminar flow with "solid-front fill" in the NVSC process (**b**)

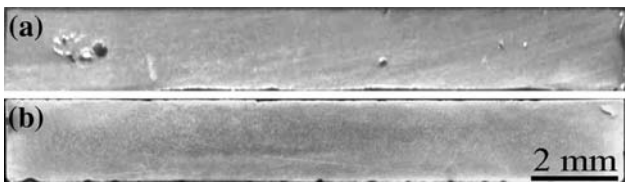

Fig. 4 Typical macroscopic cross-section appearances showing: **a** macro pores and cavities in the interior of the CVSC sheet; **b** no evident defects in the interior of the NVSC sheet

However, there was a substantial difference in macro-structural integrity between the NVSC and CVSC sheets, and as represented in Fig. 4b, no evident macro porosity occurred in the cross section of the sample.

Microstructures

A typical microstructure of the AZ91D ingot obtained by conventional solidification is shown in Fig. 5a, where well-developed primary α-Mg dendrites with β phase (the brittle intermetallic $Mg_{17}Al_{12}$) along the α-Mg grain boundaries in the form of continuous network are clearly visible, and grain size is quite large and its distribution is non-uniform due to the slower cooling rate [6]. Observation under high magnifications indicates a typical eutectic structure of the ingot, as illustrated in Fig. 5b. The microstructure consisted of primary α grains surrounded by a eutectic mixture of α-Mg and β-$Mg_{17}Al_{12}$.

Figure 6 shows the typical microstructures of the AZ91D sheets obtained by the CVSC and NVSC process at near-liquidus temperature in this investigation. It can be clearly seen that the casting process determines shape and distribution of the different phases and has a close relationship with the final microstructures.

Due to high cooling rate, the CVSC microstructures, as presented in Fig. 6a, b, exhibited very fine grains with a small amount of β-$Mg_{17}Al_{12}$ compound at the grain boundaries. Comparing Fig. 6a with b, the low-magnification imaging, there was not obvious difference in the microstructure of the sheets produced by the CVSC technology at the initial pouring temperature of 630 and 620 °C. It can be inferred that a variation of 10 °C in initial pouring temperature, decrease from 630 to 620 °C, has an insignificant effect on the resulting microstructure of the CVSC sheets. At low magnifications, due to the very small grain size, the coring was not clearly visible and it was difficult to portray the shape and distribution features of intermetallic β-$Mg_{17}Al_{12}$ phase. High-magnification imaging (Fig. 6c) represented more microstructural details. The arrangement of dendrites suggested that they were, most likely, randomly oriented with respect to each other, due to rapid and independent nucleation [16], as shown in Fig. 6c. Moreover, the porosity, observed above in macroscopic view of cross section (Fig. 4a), was also presented in the microstructure of the sample, as pointed out by arrows in Fig. 6a, c.

Figure 6d, e shows the typical microstructures of the AZ91D sheets obtained by the NVSC process at the initial pouring temperature of 630 and 620 °C, respectively. It can be seen that the NVSC AZ91D sheets exhibited the

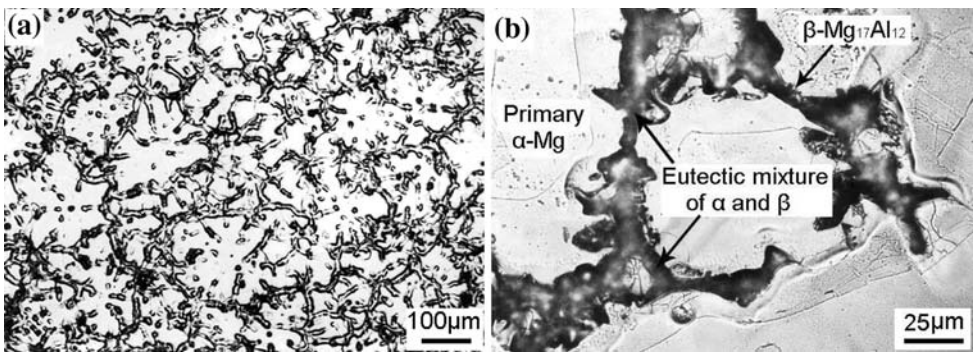

Fig. 5 Optical micrographs of the AZ91D ingot (**a**) and a typical eutectic structure (**b**)

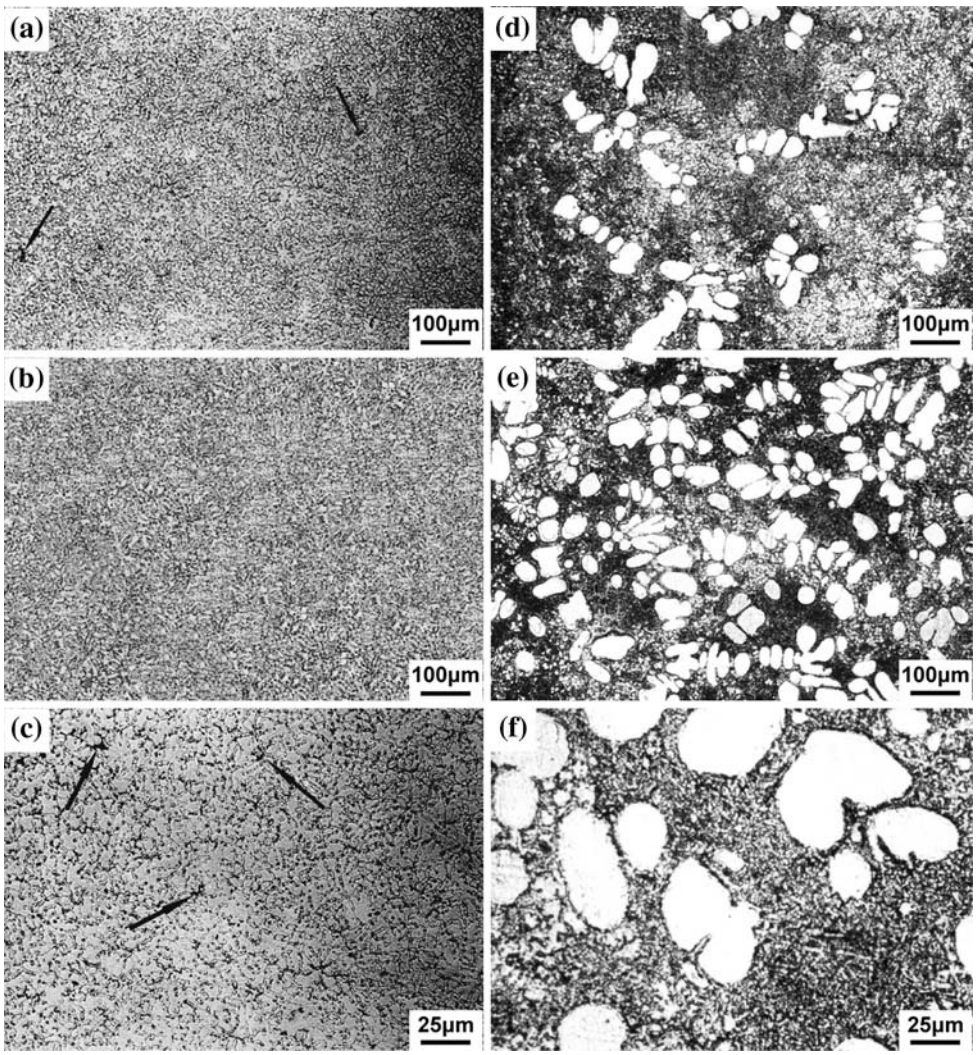

Fig. 6 Optical micrographs showing the microstructures of the AZ91D castings: **a** general view, CVSC at 630 °C; **b** general view, CVSC at 620 °C; **c** magnified view of grains and dendritic structure, CVSC at 620 °C; **d** general view of alloy containing 8% of solid particles, NVSC at 630 °C; **e** general view of alloy containing 35% of solid particles, NVSC at 620 °C; **f** a detailed morphology of primary solid particles indicating near-globular shape and degenerated rosette shape, NVSC at 620 °C

homogeneous microstructures with the primary solid α-Mg being dispersed in the matrix. The principal difference in the microstructure between the NVSC alloy and the CVSC alloy was the presence of large round or rosette solid particles of α-Mg phase that had formed during the first step of the process, i.e., when the liquid alloy passed through the shear-cooling system. Additionally, a simple visual assessment indicates that, in the NVSC process, a variation in the initial processing temperature could lead to an obvious change in solid fraction. Comparing Fig. 6d with e, in this study, when the temperature decreased from 630 to 620 °C the solid fraction increased from 8% to approximately 35%. The final primary solid size was within a range of 20 to 80 μm as examined by quantitative metallography. High-magnification imaging (Fig. 6f) revealed that the primary solid particles, exhibiting a morphology ranging from near-globules to degenerated rosettes, were surrounded by the liquid phase, which at room temperature represented practically the fine secondary α-Mg grains and the fine β-phase network [17].

The microstructural details were further imaged with SEM to examine the grain size and the final phase morphology in the microstructures of the AZ91D sheets obtained by both the processes at 620 °C, as shown in Fig. 7. It can be seen that the microstructure of the CVSC sheet comprised fine and homogeneous near-equiaxed grains, with an average size of around 7 μm in diameter, and grain boundaries were decorated by discontinuous precipitates of the intermetallic β phase (Fig. 7a). The microdistribution of major chemical elements, including Mg, Al, Zn, and Mn, within the microstructure of the CVSC alloy was much more homogeneous than that of as-cast ingot, and the microstructure dominantly consisted of supersaturated α-Mg solid solution [18]. A detailed description of the solidification process and resulting microstructure characteristics of the sheets produced by the CVSC technique can be found in Ref. [18].

The solidification occurring in the NVSC process, as a matter of fact, could be considered in two stages. The first was the nucleation and growth of the primary α-Mg in the

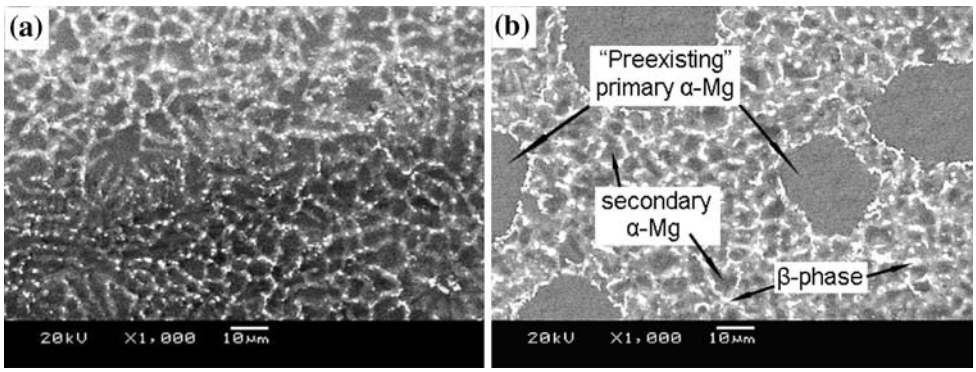

Fig. 7 SEM images showing the detailed microstructure of **a** the CVSC AZ91D sheet; **b** the NVSC AZ91D alloy produced by secondary solidification inside the mold cavity

shear-cooling system, and the second was the solidification of the liquid portion of the slurry inside the mold cavity. The whole solidification process of the NVSC technology was very similar to that of the rheo-diecasting (RDC) process described previously by Fan, et al. [17, 19–21]. Figure 7b depicts the detailed secondary solidification area in the final microstructure of the NVSC alloy. The eutectic as a mixture of fine secondary α-Mg grains and the fine β-phase, resulting from the rapid solidification of remaining liquid in the SSM slurry in the secondary solidification step, distributed around the "preexisting" primary solid particles, which had formed in the primary solidification under intensive forced convection. The secondary α-grains, delineated by the β-phase network, were morphologically of near-equiaxed shape, with an average size of about 5 μm in diameter. At this region the fine microstructure looks like that of the CVSC AZ91D alloy presented in Fig. 7a. Furthermore, the image in Fig. 7b reveals that the interface between primary α phase and the eutectic was not flat, but covered with numerous protrusions of an intermetallic compound [22]. The content of alloying elements of Al, Zn, and Mn was higher in the grain boundaries and the eutectic structure than that in the primary solid particles and in the second α-grains and thus, the mean composition of α-Mg solid solution was lower than the nominal composition of the alloy [22–24].

Phase composition

The X-ray diffraction provides information about the crystallography of phases, their contents, and an estimation of the preferred orientation. Figure 8 shows the X-ray diffraction patterns of the as-cast AZ91D ingot and the AZ91D sheets produced by both the processes at 620 °C. According to XRD measurement as shown in Fig. 8a, the AZ91D ingot contained the α-Mg and intermetallic phase of β-$Mg_{17}Al_{12}$ which was also clearly visible in its optical micrograph (Fig. 5). The CVSC sheet, molded directly from the liquid molten metal, exerted a different XRD pattern with virtually only an α-Mg phase (Fig. 8b). The anticipated locations of $Mg_{17}Al_{12}$ diffraction peaks were indicated by arrows in Fig. 8b where the peaks were not obvious and their intensities were at a very low level, and thus, the main phase of the CVSC sheet consisted of supersaturated α-Mg solid solution. The phases presented in the NVSC AZ91D alloy (Fig. 8c) were essentially the same as those obtained in foregoing as-cast ingot (Fig. 8a), which consisted of α-Mg and β-$Mg_{17}Al_{12}$ phase. However, it exhibited visually detectable lower intensities of β-$Mg_{17}Al_{12}$ peaks than that in the as-cast ingot (Fig. 8a), and higher than that after the CVSC process (Fig. 8b).

Discussion of results

Mold-filling characteristics

In contrast to liquid metal, semi-solid slurry, with fine and spheroidal particles distributed in the liquid matrix, will inevitably change the mold-filling behavior. The most important objective of SSM processing is to achieve laminar mold filling, improving surface appearances of casting sheets, and avoiding gas entrapment, by increasing the viscosity of the fed metal [19]. In this study, the filling patterns of liquid flow and SSM flow inside the mold cavity are schematically shown in Fig. 9. It can be clearly seen that the mold-filling behavior, which may directly affect the apparent morphology and the microstructure of the final casting, is very sensitive to the experimental processing conditions.

In the CVSC process, the fed liquid metal is rapidly passed through the casting runner, where the molten metal is not sufficiently cooled and thus, the molten metal is maintained in liquid state when it flows into the mold. In fact, owing to the well flowability and the high inlet velocity under vacuum pressure, the liquid alloy sprays rather than flows into the mold cavity and the mold filling is very turbulent. The mold-filling feature of liquid flow in the CVSC process is schematically exhibited in Fig. 9a. This results in the final castings with numerous radial

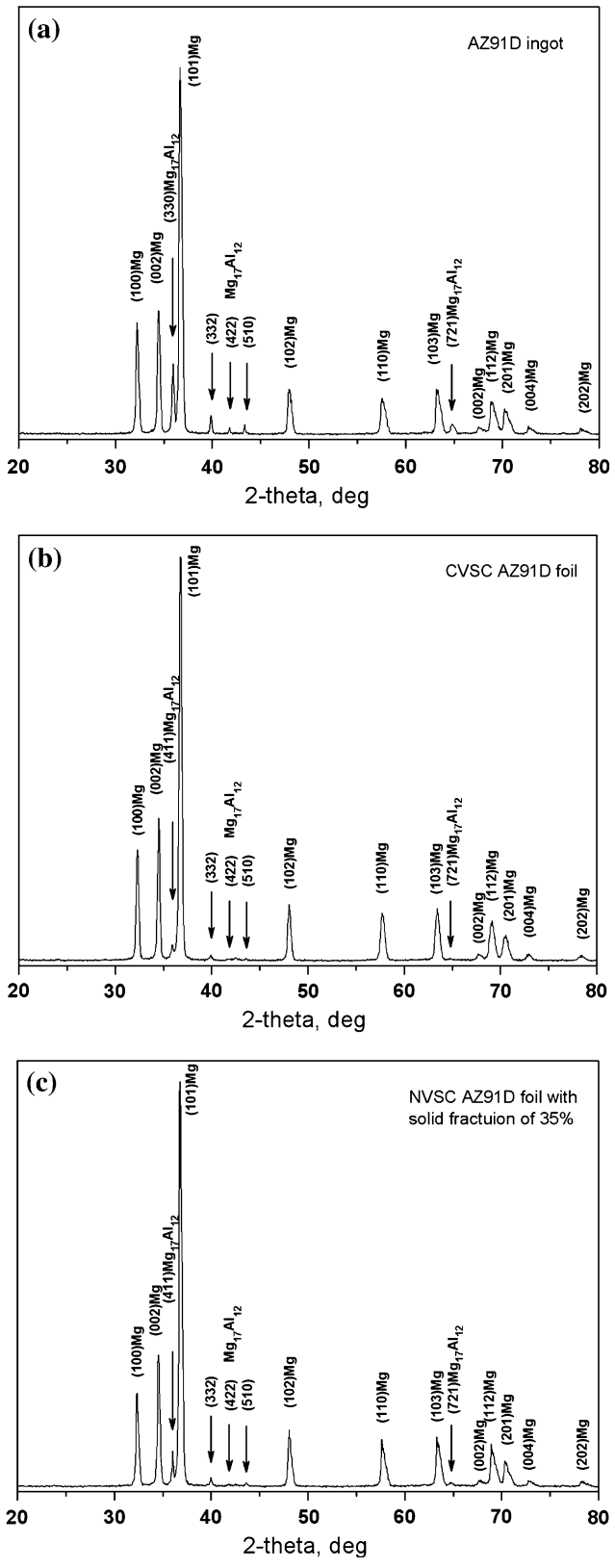

Fig. 8 X-ray diffraction patterns for AZ91D alloy: **a** as-cast ingot; **b** the CVSC sheet; **c** the NVSC sheet with solid fraction of 35%

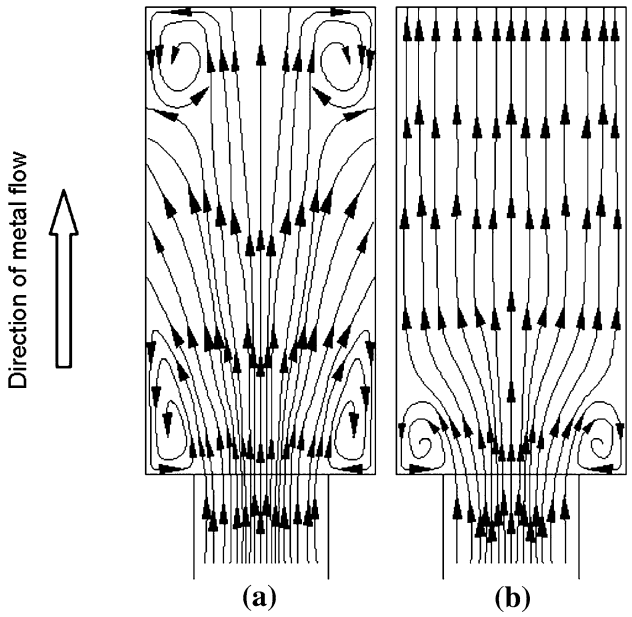

Fig. 9 Schematic of mold-filling processes of liquid metal flow (**a**) and SSM flow (**b**)

striae, jet flow traces, and the visible backflow zones on the surface (see Fig. 2a, c), accompanied by compressed gas inclusions, which may cause pores and cavities under the surface and in the sheets interior (see Fig. 4a). The regions with the porosity existing in are usually the weakest paths, susceptible to cracking. Typical SEM micrograph for fractured surface of the tensile specimen produced by the CVSC process, as shown in Fig. 10, reveals the location of pores and cavities which result from gas entrapment or solidification shrinkage. Some of them are indicated by arrows in Fig. 10a. It can be clearly seen that in this case the cracking takes place across the defects, which evidently deteriorate mechanical properties of the castings.

Mechanical stirring of an alloy during solidification has been shown to change the structure of the solidified phase from dendritic to more or less spherically shaped particles [11, 25]. In the NVSC process, the fed liquid metal is transformed to the semi-solid state by applying shear forces during the freezing process. These shear forces break up dendrites as they form during solidification and create round or rosette solid particles in the molten metal. In general, semi-solid slurry, with fine and spheroidal particles distributed uniformly in the liquid matrix, exhibits distinctive thixotropy, pseudoplasticity, and the higher viscosity as compared with liquid metal [11, 21]. Therefore, The SSM can be caused to fill the mold with "solid-front fill" [11] (Fig. 3b), as compared with the liquid metal "spraying" in the CVSC process (Fig. 3a). The smooth filling achieved in the NVSC process is schematically

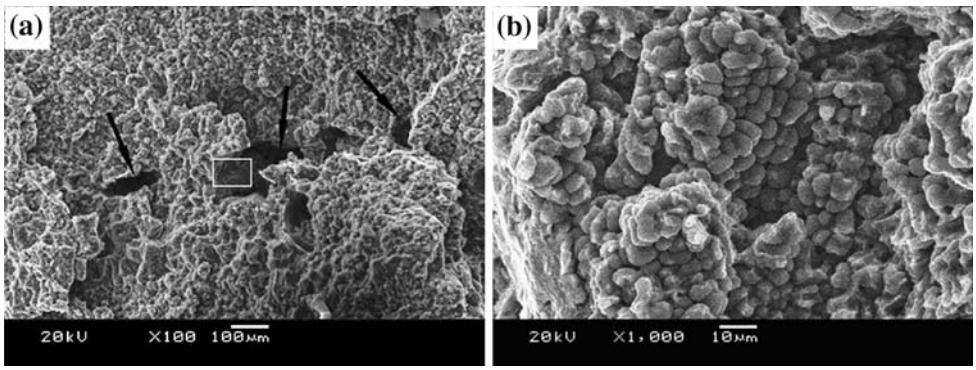

Fig. 10 SEM images of the tensile fracture surface of the AZ91D alloy produced by the CVSC process showing: **a** pores and cavities in the casting interior; **b** the detailed morphology inside the cavity

presented in Fig. 9b. Other experimental investigations [11–13, 19, 26, 27] have confirmed the effects of the semi-solid state on the flow behavior. To summarize, the beneficial changes of the mold-filling mechanism after semi-solid processing could be mainly ascribed to three aspects: (i) the lower injection molding temperature of fed metal, (ii) the higher viscosity of fed material due to increasing solid fraction of primary phase, and (iii) particle morphology and agglomeration of the semi-solid slurry. In this study, the positive effects of such semi-solid slurry on the mold-filling process have been confirmed by the experimental results represented above in Figs. 2 and 4, indicating very good surface finish (Fig. 2b, d) and the elimination of gas porosity (Fig. 4b).

Solidification behavior

The microstructure of casting is strongly influenced by the cooling rate [28, 29]. The casting process determines the volume fraction, morphology, size, and distribution of the different phases in the final microstructure [8]. The microstructure of the as-cast ingot, as shown in Fig. 5, results from a metastable solidification process: the molten metal firstly generates primary α-Mg phase with decrease in temperature; growth of divorced eutectic α-Mg adheres to the primary α-Mg; divorced eutectic β-$Mg_{17}Al_{12}$ with black contour grows into primary α-Mg; and then lamellar of secondary β-$Mg_{17}Al_{12}$ precipitates from supersaturated α-Mg [23, 28, 29]. This solidification process gives rise to a coarse and non-uniform microstructure due to the lower cooling rate (see Fig. 5), and the X-ray diffraction analyzing results indicate the high volume fraction of β phase in its microstructure (see Fig. 8a).

In the CVSC process, the molten metal into the mold cavity has an extremely high cooling rate (in the order of 10^3 K/s), which is mainly ascribed to the conjoint and mutually interactive influences of (i) the high heat transfer rate provided by the cold copper mold, (ii) the very small size of the casting, and (iii) the lower pouring temperature of fed metal (around 20–30 °C above the liquidus value). Once nucleation is triggered by the mold wall, copious heterogeneous nucleation takes place throughout the entire liquid melt with a high nucleation rate [17, 30]. Under such conditions, numerous nuclei compete to grow; each nucleus would not have much chance to grow before the liquid metal is completely consumed [19] and thus, the solidification completes even before the metastable eutectic reaction occurs, producing fine equiaxed grains in the entire volume, as shown in Figs. 7a and 10b, which exhibit the morphology inside the porosity observed by SEM, indicating the extremely finely and homogeneously distributed near-equiaxed grains in the microstructure of the CVSC sheet. Additionally, rapid solidification can obviously enlarge the solid solubility limit of alloying elements and can even form single-phase solid solution structure [31]. In the CVSC solidification process, the alloying elements in the liquid have no time to diffuse sufficiently and the high cooling rate offer a non-equilibrium solidification. As a result, the microdistribution of alloying elements, including Mg, Al, Zn, and Mn, within the microstructure of the CVSC alloy was much more homogeneous than that in the as-cast ingot [18]. Moreover, the eutectic transformation $L \rightarrow \alpha\text{-Mg} + \beta\text{-}Mg_{17}Al_{12}$, occurring in the most commercial AZ91D alloy cast processes, is suppressed to a great extent, inducing the lower proportion of β-brittle phase in the CVSC microstructure, which dominantly consists of supersaturated α-Mg solid solution (Fig. 7a). Therefore, the diffraction peaks of the β-$Mg_{17}Al_{12}$ phase in the XRD patterns of the CVSC sheet, displayed in Fig. 8b, are not obvious.

Solidification in the NVSC process takes place essentially in two stages: primary solidification, relating to the nucleation and generation of the primary solid particles of α-Mg phase when the liquid alloy was passed through the shear-cooling system, and secondary solidification, relating to the solidification of the remaining liquid in the SSM slurry inside the mold cavity, involving the formation of the fine secondary α-Mg grains and the non-equilibrium eutectic reactions.

During the primary solidification, liquid metal of temperature 20–30 °C above the liquidus value is continuously converted into the semi-solid state by applying shear forces during the freezing process. Once the nucleation temperature is reached, heterogeneous nucleation occurs in the fed liquid metal. The growth morphology of the nuclei changes from dendrites to rosettes or spheres due to the high shear rate and high intensity of turbulence [21] provided by shear-cooling system, and every single nucleus being rosette or spherical in shape will survive and contribute to the final microstructure. As the primary solidification proceeds, the alloying elements Al, Zn are enriched in the remaining liquid of SSM with the increase of the solid content of primary α-Mg phase. It should be noted that in the sub-liquidus temperature range, the solid content of the AZ91D SSM is very sensitive to the processing temperature, and a very small change in the temperature will result in substantial variation of solid fraction [30]. Therefore, in this study, an increase in solid fraction from 8% to approximately 35% takes place after reducing the initial pouring temperature by 10 °C intervals (see Fig. 6d, e). The formation mechanism of the non-dendritic structures in the SSM has been discussed by many researchers [11, 13, 27, 30, 32]. Essentially, the globular structure develops by controlling the nucleation and growth processes at the early stages of freezing [30].

The secondary solidification in the NVSC process, occurring inside the mold cavity under high cooling rate, is very similar to the solidification in the CVSC process described above. The major difference between both the solidification processes is the state of the mold-filling metal, i.e., liquid state in the CVSC process as compared with semi-solid state in the NVSC process. Once the SSM is injected into the mold cavity, nucleation would occur throughout the entire remaining liquid with a much higher nucleation rate. The high nucleation rate and the high nuclei survival rate inside the cavity ensure that each nucleus can only grow to a limited size [17], resulting in fine near-equiaxed secondary α-Mg grains, surrounded by mostly discontinuous precipitates of fine β-$Mg_{17}Al_{12}$ (Fig. 7b). According to the previous analysis, the content of alloying element Al in the remaining liquid of SSM is higher than that in the initial liquid metal due to the increase of solid fraction of primary α-Mg phase and thus, the volume fraction of the eutectic β-$Mg_{17}Al_{12}$ intermetallic phase in the NVSC sheet is higher than that in the CVSC sheet (see Fig. 8b, c). However, due to the extremely high cooling rate of the secondary solidification process, the eutectic reaction, i.e., L → α-Mg + β-$Mg_{17}Al_{12}$, is suppressed to some extent, resulting in lower volume fraction of the β-$Mg_{17}Al_{12}$ compared with that in the as-cast ingot (Fig. 8). It is generally accepted that an effective approach for better toughness is to reduce the volume fraction of the $Mg_{17}Al_{12}$ intermetallic phase [30]. Therefore, for AZ91D alloy, the NVSC process may be an alternative technology to achieve the high-integrity structure with the maximum combination of strength and ductility.

Conclusions

(1) A new semi-solid processing technique, the NVSC process, is used to manufacture high-quality components of AZ91D Mg alloy directly from a liquid metal by using the self-designed equipment. The NVSC technology combines the semi-solid slurry making and component forming operation into one step, therefore eliminating the need for specially prepared slurry and subsequent slurry transportation steps.

(2) The surface appearances of the CVSC sheets exhibit numerous radial striae, jet flow traces, and visible backflow zones. Moreover, some macro- and micro-porosities, caused by compressed gas inclusions, are presented in the interior of the CVSC sheets, whereas, the qualities of the NVSC sheets are improved significantly. It is revealed that the SSM with higher viscosity fills the mold with "solid-front fill", as compared with the liquid metal "spraying" in the CVSC process. The smooth filling achieved in the NVSC process diminishes some disadvantages inherent for the CVSC sheets, generates castings with better surface finish and structures with high integrity.

(3) In the CVSC process, the liquid metal into the mold cavity has an extremely high cooling rate, resulting in fine and homogeneous microstructure, which dominantly consists of the near-equiaxed α-Mg grains with an average size of around 7 μm in diameter. The microdistribution of alloying elements within the microstructure is much more homogeneous due to rapid solidification.

(4) Solidification in the NVSC process takes place in two distinctive stages; one is primary solidification in the shear-cooling system under high intensity of turbulence, and the other one is secondary solidification inside the mold cavity with high cooling rate. The final microstructure of the NVSC sheet exhibits that the "preexisting" primary solid particles which had formed in the primary solidification, with the morphology of near-globules or rosettes, are surrounded by the eutectic mixture of fine secondary α-Mg grains and fine precipitates of β- $Mg_{17}Al_{12}$ intermetallics, resulting from the rapid solidification of the remaining liquid of SSM in the secondary solidification step.

(5) Owing to high cooling rate, the eutectic reaction, i.e., L → α-Mg + β-$Mg_{17}Al_{12}$, is suppressed to some

extent. As a result, the volume fraction of the β-$Mg_{17}Al_{12}$ in the sheets obtained by the both processes is much lower than that in the as-cast ingot. However, the content of $Mg_{17}Al_{12}$ intermetallic phase in the NVSC sheet is slightly higher than that in the CVSC sheet.

Acknowledgements The authors are grateful for the financial support from the National Natural Science Foundation of China (Grant Nos. 50874022).

References

1. Friedrich H, Schumann S (2001) J Mater Process Technol 117:276
2. Mordike BL, Ebert T (2001) Mater Sci Eng A 302:37
3. Ambat R, Aung NN, Zhou W (2000) Corros Sci 42:1433
4. Srivatsan TS, Vasudevan S, Petraroli M (2008) J Alloys Compd 461:154
5. Eliezer D, Aghion E, Froes FH (1998) Adv Perform Mater 5:201
6. Friefrich EH, Mordike BL (2006) Magnesium technology. Springer, Berlin
7. Vogel M, Kraft O, Dehm G, Arzt E (2001) Scr Mater 45:517
8. Dahle AK, Lee YC, Nave MD, Schaffer PL, StJohn DH (2001) J Light Met 1:61
9. El-Mahallawy NA, Taha MA, Pokora E, Klein F (1998) J Mater Process Technol 73:125
10. Kleiner S, Beffort O, Wahlen A, Uggowitzer PJ (2002) J Light Met 2:277
11. Flemings MC (1991) Metall Mater Trans A 22:957
12. Kirkwood DH (1994) Int Mater Rev 39:173
13. Fan Z (2002) Int Mater Rev 47:49
14. Rice CS, Mendez PF (2001) Adv Mater Process 159:49
15. Okamoto H (1998) J Phase Equilib 19:598
16. Czerwinski F (2002) Acta Mater 50:3265
17. Wang Y, Liu G, Fan Z (2006) Acta Mater 54:689
18. Teng H, Zhang X, Zhang Z, Li T, Cockcroft S (2009) Mater Charact 60:482
19. Fan Z (2005) Mater Sci Eng A 413–414:72
20. Fan Z, Liu G (2005) Acta Mater 53:4345
21. Ji S, Fan Z, Bevis MJ (2001) Mater Sci Eng A 299:210
22. Czerwinski F, Zielinska-Lipiec A, Pinet PJ, Overbeeke J (2001) Acta Mater 49:1225
23. Zhang X, Li T, Teng H, Xie S, Jin J (2008) Mater Sci Eng A 475:194
24. Mathieu S, Rapin C, Hazan J, Steinmetz P (2002) Corros Sci 44:2737
25. Mada M, Ajersch F (1996) Mater Sci Eng A 212:157
26. Modigell M, Koke J (2001) J Mater Process Technol 111:53
27. Atkinson HV (2005) Prog Mater Sci 50:341
28. Song G, Atrens A, Dargusch M (1999) Corros Sci 41:249
29. Cai J, Ma GC, Liu Z, Zhang HF, Hu ZQ (2006) J Alloys Compd 422:92
30. Czerwinski F (2005) Acta Mater 53:1973
31. Minkoff I (1986) Solidification and cast structure. Wiley, New York
32. Mullis AM (1999) Acta Mater 47:1783